Applied Physics Letters

RESEARCH ARTICLE | APRIL 16 2026

Elliptical acoustic resonator-enabled synchronous acoustic excitation by multiple laser beams in quartz-enhanced photoacoustic spectroscopy

Ruyue Cui; Zimu Wang; Wenfei Han; Yingzhang Ren; Chunxia Li; Jiale Xu; Xinran Li; Vincenzo Spagnolo ; Weidong Chen; Hongpeng Wu ; Lei Dong

Appl. Phys. Lett. 128, 152203 (2026)
https://doi.org/10.1063/5.0322692

Applied Physics Letters ARTICLE pubs.aip.org/aip/apl

Elliptical acoustic resonator-enabled synchronous acoustic excitation by multiple laser beams in quartz-enhanced photoacoustic spectroscopy

Cite as: Appl. Phys. Lett. **128**, 152203 (2026); doi: 10.1063/5.0322692
Submitted: 13 January 2026 · Accepted: 25 March 2026 ·
Published Online: 16 April 2026

Ruyue Cui,[1,2,3] Zimu Wang,[1,2] Wenfei Han,[1,2] Yingzhang Ren,[1,2] Chunxia Li,[1,2] Jiale Xu,[1,2] Xinran Li,[1,2] Vincenzo Spagnolo,[4] Weidong Chen,[3] Hongpeng Wu,[1,2,a)] and Lei Dong[1,2,a)]

AFFILIATIONS

[1]State Key Laboratory of Quantum Optics Technologies and Devices, Institute of Laser Spectroscopy, Shanxi University, Taiyuan 030006, China
[2]Collaborative Innovation Center of Extreme Optics, Shanxi University, Taiyuan 030006, China
[3]Laboratoire de Physico-chimie de l'Atmosphère, Université du Littoral Côte d'Opale, Dunkerque 59140, France
[4]PolySense Lab—Dipartimento Interateneo di Fisica, University and Politecnico of Bari, Bari, Italy

[a)]**Authors to whom correspondence should be addressed:** wuhp@sxu.edu.cn and donglei@sxu.edu.cn

ABSTRACT

We report synchronous excitation of an acoustic mode in quartz-enhanced photoacoustic spectroscopy (QEPAS) enabled by an elliptical acoustic resonator under multi-beam illumination. In this configuration, multiple laser beams distributed within the prong gap of a quartz tuning fork (QTF) coherently excite the same acoustic mode, leading to efficient acoustic energy confinement and enhanced coupling to the QTF. Finite-element simulations based on distributed line acoustic sources reveal that, compared with the resonator-free case, a half-wavelength acoustic resonator enhances the effective acoustic excitation by a factor of approximately 4, while a three-quarter-wavelength resonator provides a higher enhancement of about 7. These predictions are experimentally validated using a multi-pass cell-based QEPAS system incorporating an elliptical acoustic resonator. The results demonstrate that resonator-enabled synchronous multi-beam excitation reshapes the acoustic coupling behavior in QEPAS and provides a practical route toward high-sensitivity photoacoustic sensing beyond optical field-limited enhancement.

Gas analysis plays an important role in atmospheric science, space science, and medical diagnostics,[1–3] driving sustained demand for gas-sensing technologies with high sensitivity, good selectivity, and low cost.[4–6] Among various optical sensing techniques, quartz-enhanced photoacoustic spectroscopy (QEPAS) has attracted significant attention due to its high sensitivity, compact configuration, and strong immunity to environmental noise.[7,8] In QEPAS, a quartz tuning fork (QTF) with a high-quality factor is employed as an acoustic-to-electrical transducer to efficiently detect sound waves generated by the photoacoustic effect.

The sensitivity of QEPAS is fundamentally governed by the strength of the photoacoustic field and the efficiency of acoustic coupling to the QTF.[9,10] Since photoacoustic waves are generated along the excitation laser path, while the QTF is the most sensitive to acoustic fields confined within its prong gap,[11–13] enhancing the effective photoacoustic excitation in this region has been a central strategy for improving QEPAS performance. On this basis, multiple-sound-source-excitation QEPAS (MSSE-QEPAS) schemes have been proposed, in which multiple laser beams produced by multi-pass cell configurations generate distributed photoacoustic sources within the QTF prong gap, leading to significant signal enhancement.[14]

However, in MSSE-QEPAS systems, the effective acoustic sensing volume of the QTF remains fundamentally constrained by the prong thickness, which is typically on the order of 300 μm. As a result, only photoacoustic sources generated within this narrow region can be efficiently detected, and further signal enhancement becomes increasingly limited when relying solely on optical field manipulation,[15,17–19] such as increasing the number of laser passes. Since photoacoustic waves are generated continuously along the excitation laser path, an effective strategy to overcome this limitation is to collect and confine the distributed acoustic energy and subsequently couple it efficiently to the QTF. Acoustic resonators provide a natural means to enhance acoustic confinement and coupling in QEPAS systems.[20] While the coupling mechanisms of cylindrical acoustic resonators have been extensively

studied in conventional single-sound-source QEPAS configurations,[21–23] recent studies have also explored multi-pass and multi-source photoacoustic configurations with engineered acoustic resonators, primarily in conventional PAS systems.[25,26] However, the direct application of these mechanisms to MSSE-QEPAS is nontrivial due to the more complex acoustic field distribution arising from multiple distributed excitation beams. In particular, how to engineer the resonator geometry to enable efficient and synchronous excitation of a well-defined acoustic mode under multi-beam illumination remains largely unexplored.

In this work, we report synchronous multi-beam excitation of an acoustic mode in QEPAS enabled by an elliptical acoustic resonator. By confining multiple coplanar photoacoustic sources within an elliptical resonator matched to the spatial distribution of the excitation beams, the efficient acoustic energy confinement and the enhanced coupling to the QTF are achieved. Finite-element simulations based on distributed line acoustic sources are performed to analyze the acoustic field distribution and resonator coupling behavior, and the numerical predictions are validated experimentally using a multi-pass cell-based QEPAS system. The results reveal that resonator geometry plays a critical role in governing acoustic coupling under multi-beam excitation and provide new insight into acoustic mode engineering for advanced QEPAS sensors.

To elucidate the mechanism of synchronous acoustic excitation under multi-beam illumination, a finite-element model of a QEPAS system incorporating an elliptical acoustic resonator was established, as shown in Fig. 1. In the model, multiple coplanar line acoustic sources are introduced to represent distributed photoacoustic excitation generated by multiple laser beams within the QTF prong gap [Fig. 1(a)]. This line-source representation serves as an effective approximation of the distributed volumetric photoacoustic excitation, given the small beam diameter relative to the acoustic wavelength and the characteristic dimensions of the resonator. Since these sources pass through the acoustically sensitive region of the QTF, the resulting acoustic interaction is predominantly governed by the sound field in the y–z plane. An elliptical acoustic resonator is, therefore, employed [Fig. 1(b)] to spatially match the planar distribution of the photoacoustic sources. The major and minor axes of the elliptical resonator are chosen to be slightly larger than the transverse extent of the excitation beam distribution in the cross section, ensuring effective acoustic confinement without obstructing laser beam propagation. In addition, a narrow slit is reserved at the center of the resonator cross section to enable non-contact acoustic coupling between the QTF and the resonator. Compared with conventional cylindrical resonators used in single-beam QEPAS configurations, the elliptical geometry enables more efficient confinement of acoustic energy generated by coplanar sources and facilitates their synchronous coupling to a well-defined acoustic mode. In contrast, conventional cylindrical resonators are primarily optimized for single-beam excitation and do not provide spatial matching for distributed multi-beam photoacoustic sources. A y–z cross-sectional view of the coupled system is shown in Fig. 1(c), where the resonator length L is varied to examine its role in establishing constructive acoustic coupling, while all other parameters are fixed.

Figures 1(d)–1(f) present the simulated acoustic pressure distributions for three representative configurations: without a resonator, with a half-wavelength resonator, and with a three-quarter-wavelength resonator. Here, the wavelength corresponds to the acoustic wavelength associated with the QTF resonance frequency ($f_0 = 7.2$ kHz). Without an acoustic resonator, the acoustic field generated by distributed sources is weakly confined and spreads over a broad spatial region, resulting in inefficient excitation of the QTF. In contrast, the introduction of an elliptical resonator leads to pronounced acoustic

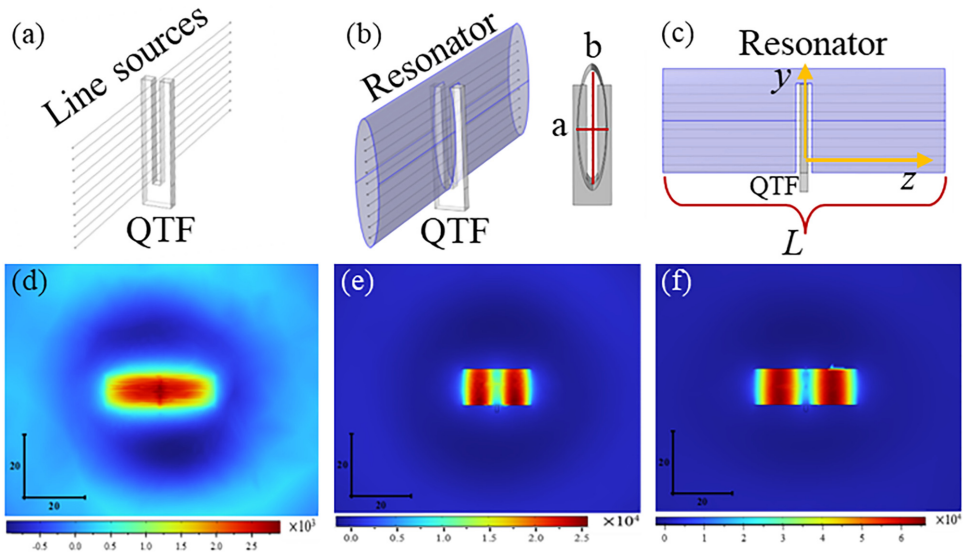

FIG. 1. Numerical model and simulated acoustic fields illustrating resonator-enabled synchronous excitation in a multi-beam QEPAS system. (a) Distributed coplanar line acoustic sources representing photoacoustic excitation generated by multiple laser beams within the QTF prong gap. (b) Elliptical acoustic resonator designed to spatially match the planar distribution of the photoacoustic sources and enable efficient acoustic confinement. (c) y–z cross-sectional view of the coupled QTF–resonator system, where the resonator length L is varied while other geometric parameters are fixed. (d)–(f) Simulated acoustic pressure distributions in the y–z plane showing acoustic mode formation for (d) the resonator-free configuration, (e) a half-wavelength resonator, and (f) a three-quarter-wavelength resonator.

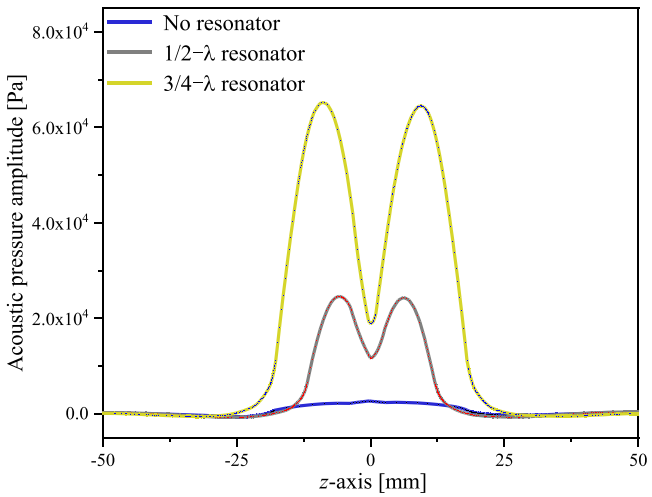

FIG. 2. Simulated acoustic pressure amplitude along the *z* axis at the center of the QTF prong gap for different resonator configurations, illustrating resonator-enabled synchronous excitation of distributed photoacoustic sources.

confinement within the prong gap. Notably, different resonator lengths give rise to distinct acoustic mode structures, indicating that the resonator geometry governs whether distributed photoacoustic sources can synchronously excite the same acoustic mode.

To quantitatively assess the effectiveness of synchronous acoustic excitation, the acoustic pressure amplitude along the *z* axis passing through the center of the QTF prong gap was extracted, as shown in Fig. 2. Owing to the geometric symmetry and coplanar source distribution, this profile provides a representative measure of effective acoustic excitation experienced by the QTF. The results show that the three-quarter-wavelength resonator produces the highest acoustic pressure at the prong gap center, corresponding to the most efficient constructive superposition of acoustic waves generated by distributed sources. This behavior indicates that appropriate resonator geometry enables synchronous excitation of a single acoustic mode, rather than merely increasing local acoustic intensity.

The experimental setup used to validate the numerical predictions is shown in Fig. 3. A QTF with a resonance frequency of 7.205 kHz and a quality factor of approximately 8500 was employed. The QTF has a prong length of 10 mm and a prong spacing of 800 μm, which is larger than the laser beam diameter of 600 μm, ensuring unobstructed laser propagation through the prong gap. Multi-sound-source excitation was realized using a multi-pass cell (MPC). A single laser beam was repeatedly reflected between two spherical mirrors with curvature radii of 100 mm and a separation of 36.6 mm. With an incident beam diameter of ∼0.6 mm and an injection angle of ∼5°, a single-line beam pattern was formed and confined within the QTF prong gap. Under this configuration, ∼60 beam passes were achieved within a projected area of ∼8 mm^2, resulting in spatially distributed photoacoustic excitation sources. The QTF was positioned inside the MPC such that all laser passes overlapped with its acoustically sensitive region. An elliptical acoustic resonator, fabricated according to the numerical model, was integrated to enable synchronous acoustic coupling, which introduces additional acoustic loading and leads to a slight reduction in the effective Q-factor while improving the acoustic coupling efficiency.[24] The major axis of the resonator was 11.8 mm, slightly exceeding the QTF prong length to fully cover the transverse distribution of the multiple sound sources along the *y* direction, while the minor axis was set to 1 mm, marginally larger than the prong spacing to allow unobstructed laser transmission while maintaining effective acoustic confinement. The resonator length was configured to be either one-half or three-quarters of the acoustic wavelength, with the acoustic resonance frequency matched to that of the QTF. Due to the limited cavity length (36.6 mm) of the MPC configuration, a full-wavelength resonator was not considered. A narrow slit was machined at the center of the resonator to accommodate the QTF without mechanical contact, enabling efficient acoustic

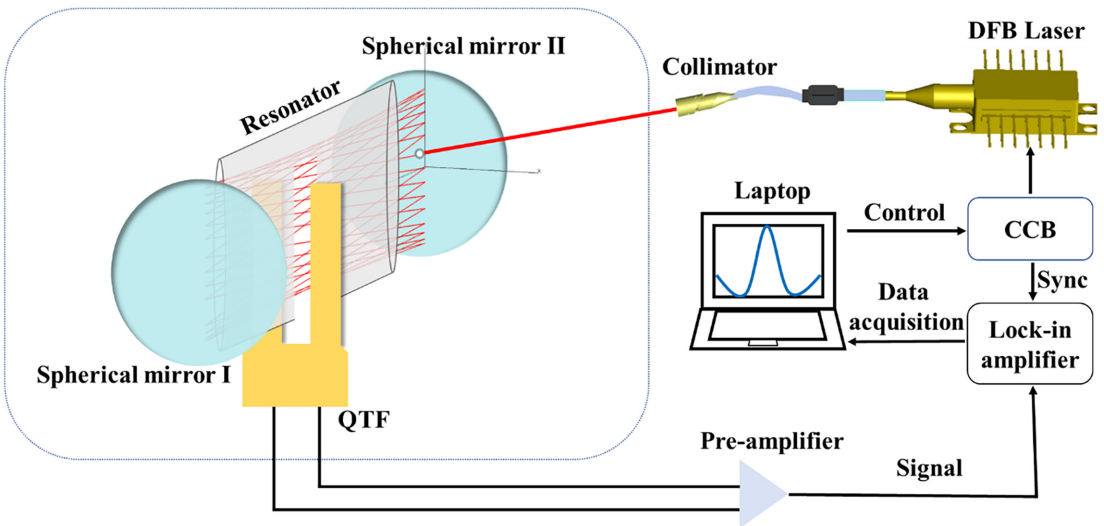

FIG. 3. Experimental setup enabling synchronous multi-beam acoustic excitation in QEPAS using a MPC and an elliptical acoustic resonator coupled to a QTF.

coupling while avoiding mechanical interference. A continuous-wave distributed feedback (DFB) laser operating at 1.395 μm was used as the excitation source, targeting a water vapor absorption line at 7181.15 cm^{-1}. The optical output power was 16 mW, and the ambient water vapor concentration during the experiments was approximately 8500 ppm. Wavelength modulation spectroscopy with the second harmonic ($2f$) detection was employed, and the QTF signal was demodulated using a lock-in amplifier with a time constant of 1 s and a filter slope of 12 dB/octave.

Figure 4 compares the measured $2f$ photoacoustic signal amplitudes obtained under four representative configurations: conventional single-beam QEPAS, multi-beam QEPAS without an acoustic resonator, and multi-beam QEPAS coupled with half-wavelength and three-quarter-wavelength elliptical acoustic resonators. Compared with the conventional single-beam configuration, multi-beam excitation yields a signal enhancement factor of approximately 16.9, confirming that distributed photoacoustic sources within the QTF prong gap significantly increase the effective acoustic excitation. This enhancement does not scale linearly with the number of beams due to the position-dependent acoustic response of the QTF.[16]

Upon introducing the elliptical acoustic resonator, further signal enhancement is observed, reflecting improved acoustic confinement and coupling. Notably, the three-quarter-wavelength resonator produces a substantially higher enhancement (~6.8) than the half-wavelength resonator (~3.6) relative to the resonator-free case. This behavior is consistent with numerical predictions in Fig. 2, which indicate that the three-quarter-wavelength geometry enables more efficient constructive superposition of acoustic waves generated by distributed coplanar sources. The experimentally measured enhancement factors agree with simulated values (3.9 and 6.7, respectively) within 10%, confirming that the finite-element model captures the dominant acoustic coupling behavior. These results demonstrate that, under multi-beam excitation, the signal enhancement is governed not solely by the resonator length but by the ability of the resonator geometry to enable synchronous excitation of a well-defined acoustic mode. Although the optimal resonator length lies within the range commonly reported for conventional single-beam QEPAS systems, the underlying enhancement mechanism in the present configuration arises from resonator-enabled acoustic mode engineering rather than simple acoustic amplification. As a result, the three-quarter-wavelength elliptical resonator provides more favorable acoustic coupling than the half-wavelength resonator, in agreement with both numerical and experimental observations.

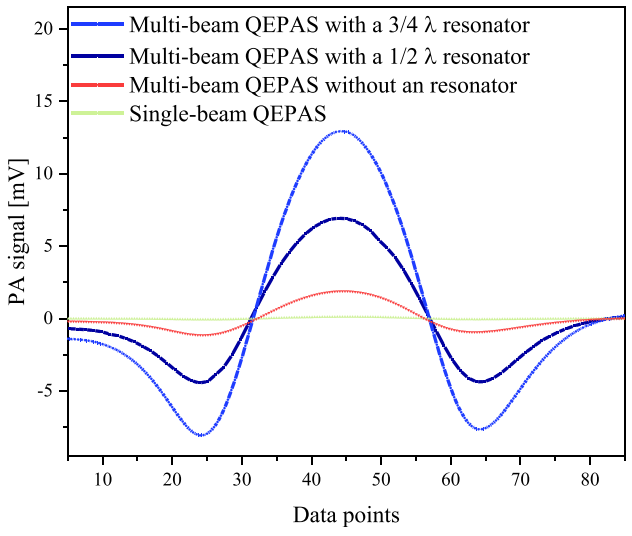

FIG. 4. Measured $2f$ photoacoustic signal amplitudes demonstrating resonator-enabled synchronous excitation under multi-beam illumination in QEPAS.

In conclusion, we demonstrate synchronous acoustic mode excitation enabled by an elliptical resonator in a multi-beam QEPAS system. By confining distributed photoacoustic sources within a resonator geometry matched to their spatial distribution, enhanced acoustic coupling to the QTF is achieved. The resulting signal enhancement, reaching approximately sevenfold for a three-quarter-wavelength resonator, arises from resonator-enabled mode synchronization rather than conventional acoustic amplification. These findings highlight acoustic mode engineering as a powerful approach for advancing multi-beam photoacoustic spectroscopy.

The project was sponsored by the National Key R&D Program of China (No. 2025ZD1200704); the National Natural Science Foundation of China (NSFC) (Nos. 62505163, 62235010, 62501370, 62475137, and 62405042); the Fundamental Research Program of Shanxi Province, China (Nos. 202403021212183 and 202303021222034); the Scientific and Technological Innovation Programs of Higher Education Institutions in Shanxi Province of China (No. 2024L014); the Research Project Supported by Shanxi Scholarship Council of China (No. 2025-060); and the Shanxi Provincial Special Fund for Scientific and Technological Cooperation and Exchange (Nos. 202404041101022 and 202304041101019).

AUTHOR DECLARATIONS

Conflict of Interest

The authors have no conflicts to disclose.

Author Contributions

Ruyue Cui and Zimu Wang contributed equally to this work.

Ruyue Cui: Data curation (equal); Formal analysis (equal); Funding acquisition (equal); Investigation (equal); Methodology (equal); Software (equal); Validation (equal); Writing – original draft (equal). **Zimu Wang:** Data curation (equal); Formal analysis (equal); Investigation (equal); Software (equal); Validation (equal). **Wenfei Han:** Investigation (equal); Software (equal); Validation (equal). **Yingzhang Ren:** Data curation (equal); Software (equal); Validation (equal). **Chunxia Li:** Formal analysis (equal); Software (equal). **Jiale Xu:** Formal analysis (equal); Investigation (equal); Software (equal). **Xinran Li:** Investigation (equal); Software (equal); Validation (equal). **Vincenzo Spagnolo:** Investigation (equal); Supervision (equal); Validation (equal). **Weidong Chen:** Supervision (equal); Validation (equal). **Hongpeng Wu:** Funding acquisition (equal); Methodology (equal); Writing – review & editing (equal). **Lei Dong:** Data curation (equal); Formal analysis (equal); Funding acquisition (equal); Investigation (equal); Methodology (equal); Supervision (equal); Writing – review & editing (equal).

DATA AVAILABILITY

The data that support the findings of this study are available within the article.

REFERENCES

[1]X. Zhao, H. Wang, Y. Xu, C. Li, H. Qi, M. Guo, W. Peng, and K. Chen, Appl. Phys. Lett. **126**, 174101 (2025).
[2]K. Kinjalk, F. Paciolla, B. Sun, A. Zifarelli, G. Menduni, M. Giglio, H. Wu, L. Dong, D. Ayache, D. Pinto, A. Vicet, A. Baranov, P. Patimisco, A. Sampaolo, and V. Spagnolo, Appl. Phys. Rev. **11**, 021427 (2024).
[3]S. Zhu, H. Wang, C. Sun, X. Zhao, H. Qi, Y. Xu, C. Li, X. Wang, and K. Chen, J. Anal. Test. **10**, 273–283 (2025).
[4]R. Cui, W. Han, C. Wang, C. Li, Y. Ren, X. Li, J. Xu, V. Spagnolo, W. Chen, H. Wu, and L. Dong, Photoacoustics **48**, 100811 (2026).
[5]H. Lin, C. Wang, L. Lin, M. Wang, W. Zhu, Y. Zhong, J. Yu, F. K. Tittel, and H. Zheng, Appl. Phys. Lett. **122**, 111101 (2023).
[6]R. Cui, Y. Yuan, S. Qui, W. Han, J. Huang, L. Wang, H. Wu, W. Chen, and L. Dong, Anal. Chem. **97**, 13095–13102 (2025).
[7]H. Wu, L. Dong, H. Zheng, Y. Yu, W. Ma, L. Zhang, W. Yin, L. Xiao, S. Jia, and F. K. Tittel, Nat. Commun. **8**, 15331 (2017).
[8]Y. Ma, S. Qiao, R. Wang, Y. He, C. Fang, and T. Liang, Appl. Phys. Rev. **11**, 041412 (2024).
[9]Q. Nie, Z. Wang, S. Borri, P. De Natale, and W. Ren, Appl. Phys. Lett. **123**, 054102 (2023).
[10]P. Patimisco, A. Sampaolo, L. Dong, F. K. Tittel, and V. Spagnolo, Appl. Phys. Rev. **5**, 011106 (2018).
[11]J. Wang, H. Wu, A. Sampaolo, P. Patimisco, V. Spagnolo, S. Jia, and L. Dong, Light: Sci. Appl. **13**, 77 (2024).
[12]T. Liang, S. Qiao, Y. Chen, Y. He, and Y. Ma, Photoacoustics **36**, 100592 (2024).
[13]F. Sgobba, A. Sampaolo, P. Patimisco, M. Giglio, G. Menduni, A. C. Ranieri, C. Hoelzl, H. Rossmadl, C. Brehm, V. Mackowiak, D. Assante, E. Ranieri, and V. Spagnolo, Photoacoustics **25**, 100318 (2022).
[14]S. Borri, P. Patimisco, I. Galli, D. Mazzotti, G. Giusfredi, N. Akikusa, M. Yamanishi, G. Scamarcio, P. De Natale, and V. Spagnolo, Appl. Phys. Lett. **104**, 091114 (2014).
[15]H. Zheng, L. Dong, P. Patimisco, H. Wu, A. Sampaolo, X. Yin, S. Li, W. Ma, L. Zhang, W. Yin, L. Xiao, V. Spagnolo, S. Jia, and F. K. Tittel, Appl. Phys. Lett. **110**, 021110 (2017).
[16]R. Cui, H. Wu, L. Dong, W. Chen, and F. K. Tittel, Appl. Phys. Lett. **118**, 161101 (2021).
[17]R. Cui, L. Dong, H. Wu, S. Li, X. Yin, L. Zhang, W. Ma, W. Yin, and F. K. Tittel, Opt. Lett. **44**, 1108 (2019).
[18]R. Cui, L. Dong, H. Wu, W. Chen, and F. K. Tittel, Appl. Phys. Lett. **116**, 091103 (2020).
[19]S. Qiao, Y. Ma, P. Patimisco, A. Sampaolo, Y. He, Z. Lang, F. K. Tittel, and V. Spagnolo, Opt. Lett. **46**, 977–980 (2021).
[20]L. Dong, A. A. Kosterev, D. Thomazy, and F. K. Tittel, Appl. Phys. B **100**, 627–635 (2010).
[21]A. A. Kosterev, Y. A. Bakhirkin, F. K. Tittel, S. McWhorter, and B. Ashcraft, Appl. Phys. B **92**, 103–109 (2008).
[22]H. Wu, A. Sampaolo, L. Dong, P. Patimisco, X. Liu, H. Zheng, X. Yin, W. Ma, L. Zhang, W. Yin, V. Spagnolo, S. Jia, and F. K. Tittel, Appl. Phys. Lett. **107**, 111104 (2015).
[23]B. Li, X. Yang, Z. Sun, J. Wang, P. Zheng, and X. Yin, Sens. Actuators, B **443**, 138317 (2025).
[24]P. Patimisco, G. Scamarcio, F. K. Tittel, and V. Spagnolo, Sensors **14**(4), 6165–6206 (2014).
[25]G. Guo, L. Li, Y. Zhou, T. Gong, Y. Tian, X. Sun, J. Cui, S. Shi, Z. Guo, X. He, X. Qiu, J. Sun, C. Jiang, C. Fittschen, and C. Li, Anal. Chem. **96**(19), 7730–7737 (2024).
[26]Y. Wu and P. Luo, Anal. Chem. **97**(6), 3302–3309 (2025).